



Short communication

Synthesis and inhibition study of monoamine oxidase, indoleamine 2,3-dioxygenase and tryptophan 2,3-dioxygenase by 3,8-substituted 5H-indeno[1,2-c]pyridazin-5-one derivatives

J. Reniers^{a,*}, C. Meinguet^a, L. Moineaux^a, B. Masereel^b, S.P. Vincent^c, R. Frederick^{a,b}, J. Wouters^{a,**}

^aDrug Design and Discovery Center, Laboratoire de Chimie Biologique Structurale, Member of NARILIS, Facultés Universitaires Notre-Dame de la Paix, Namur, Belgium

^bDrug Design and Discovery Center, Département de Pharmacie, Member of NARILIS, Facultés Universitaires Notre-Dame de la Paix, Namur, Belgium

^cLaboratoire de Chimie Bio-Organique, Facultés Universitaires Notre-Dame de la Paix, Namur, Belgium

ARTICLE INFO

Article history:

Received 21 February 2011

Received in revised form

16 September 2011

Accepted 22 September 2011

Available online 8 October 2011

Keywords:

5H-indeno[1,2-c]pyridazin-5-one

Monoamine oxidase (MAO)

Indoleamine 2,3-dioxygenase (IDO)

Tryptophan 2,3-dioxygenase (TDO)

Docking

X-ray

ABSTRACT

Previous studies on 5H-indeno[1,2-c]pyridazin-5-one derivatives as inhibitors of MAO-B revealed that it was possible to increase the MAO-B inhibitory potency of 5H-indeno[1,2-c]pyridazin-5-ones by substituting the central heterocycle in the 3-position or C-8 with lipophilic groups which occupy the substrate cavity or the entrance of the binding site, respectively. Here, four new 5H-indeno[1,2-c]pyridazin-5-one derivatives containing lipophilic groups at both positions were synthesized and their inhibitory potency against human monoamine oxidase A and B were evaluated. Selectivity of these compounds against IDO and TDO, two enzymes sharing substrate similarity with MAO and involved in the serotonergic and kynurenine pathways was also studied. All compounds showed higher activity and selectivity against MAO-B, the most effective one being 3-methyl-8-*meta*-chlorobenzyloxy-5H-indeno[1,2-c]pyridazin-5-one (**9a**) which was shown to be a competitive inhibitor with a K_i value of 0.11 μ M. Replacing the methyl group in the 3-position with a *meta*-CF₃-phenyl group (**7a**, **7b** and **7c**) abolished the inhibitory potency against MAO-B. Indeed, the substitution of the 5H-indeno[1,2-c]pyridazin-5-one core in the 3-position dramatically influences the MAO-inhibiting properties of these compounds. Molecular docking studies of **9a** within MAO-B suggest that the 5H-indeno[1,2-c]pyridazin-5-one scaffold is well stabilized into the substrate cavity with the *meta*-chlorobenzyloxy side chain extending towards a rather hydrophobic pocket at the entrance cavity.

© 2011 Elsevier Masson SAS. All rights reserved.

1. Introduction

Monoamine oxidase (MAO) is a flavoenzyme with the flavin adenine dinucleotide (FAD) covalently bound to a cysteine residue by a 8 α -(*S*-cysteinyl)-thioether linkage. The enzyme is anchored to the mitochondrial outer membrane of neuronal, glial and several other cell types. It catalyzes the oxidative deamination of biogenic and xenobiotic amines to the corresponding aldehyde and ammonia in the periphery as well as in the central nervous system [1]. In mammals, MAO exists in two isoforms, MAO-A and MAO-B. Both enzymes are dimeric in their membrane bound forms. Human MAO-A (hMAO-A) and MAO-B (hMAO-B) are encoded by separate genes and their amino acid sequences are ~70% identical [2].

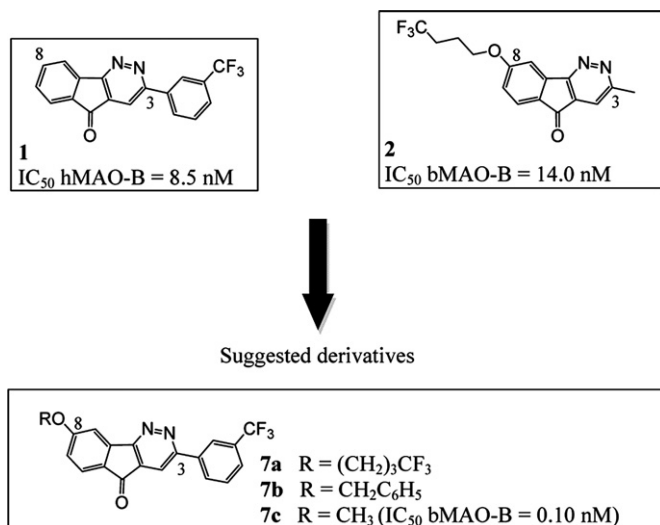
However, their distribution within the body and their substrate/inhibitor specificity are significantly different [3–5]. MAO-A preferentially catalyzes the deamination of serotonin, adrenaline, and noradrenaline, and is selectively inhibited by clorgyline and moclobemide; MAO-B preferentially catalyzes the deamination of β -phenylethylamine and benzylamine, and is irreversibly inhibited by selegiline. *In vitro*, dopamine and tyramine are deaminated by both isoforms, but dopamine *in vivo* is preferentially metabolized by MAO-B.

MAO-A and MAO-B are attractive targets for therapeutic intervention. MAO-A inhibitors are used for the treatment of mental depression and anxiety [6] whereas MAO-B inhibitors are used with L-DOPA and/or dopamine agonists in the symptomatic treatment of Parkinson's disease [7,8]. However, most of the current monoamine oxidase inhibitors lead to side effects by a lack of affinity and selectivity towards one of the isoforms. Therefore, the finding of reversible and selective inhibitors of MAO-A and MAO-B remains an important problem. In this context, we addressed this question and designed novel potent MAO inhibitors.

* Corresponding author. Tel.: +32 81 724569; fax: +32 81 725440.

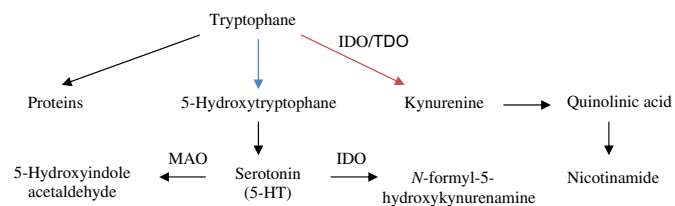
** Corresponding author. Tel.: +32 81 724550; fax: +32 81 725440.

E-mail addresses: jeremy.reniers@fundp.ac.be (J. Reniers), johan.wouters@fundp.ac.be (J. Wouters).



Scheme 1. Rational design of new 5*H*-indeno[1,2-*c*]pyridazin-5-one analogues.

Previous studies on 5*H*-indeno[1,2-*c*]pyridazin-5-one derivatives as inhibitors of MAO-B revealed that the substitution of 5*H*-indeno[1,2-*c*]pyridazin-5-one scaffold in the 3-position with lipophilic and bulky groups such *meta*-CF₃-phenyl (**1**, IC₅₀ hMAO-B = 8.5 nM [9], **Scheme 1**) increases the MAO-B inhibitory potency of this series [9,10]. Molecular docking studies suggest that the *meta*-CF₃-phenyl occupies the substrate cavity (**Fig. 1**) [9]. Further studies also revealed that the substitution in the 8-position of the central heterocycle with lipophilic and bulky groups such trifluorobutyloxy (**2**, IC₅₀ baboon MAO-B (bMAO-B) = 14.0 nM [11], **Scheme 1**) increases the MAO-B inhibitory potency of this series [11,12]. Docking studies suggest that this trifluorobutyloxy side chain occupies the entrance cavity (**Fig. 1**) [12]. Interestingly, the inhibitory activity reported by Frederick et al. on derivative **7c** (IC₅₀



Scheme 2. Pathways of tryptophan metabolism. Of the dietary tryptophan that is not used in protein synthesis, 99% is metabolized along the kynurenine pathway (red arrows). Alternative pathway is the conversion of tryptophan to serotonin (5-HT) (serotonergic pathway, blue arrows) [14]. (For interpretation of the references to colour in this figure legend, the reader is referred to the web version of this article).

bMAO-B = 0.10 nM, **Scheme 1**) bearing *meta*-CF₃-phenyl and methoxy groups in the 3- and 8-positions, respectively [11] leads us to synthesize new 5*H*-indeno[1,2-*c*]pyridazin-5-one derivatives containing lipophilic and bulky groups at both positions (**7a–b**, **Scheme 1**) including **7c** as a reference drug. In addition, the synthesis of two new compounds (**9a–b**) structurally related to compound **2** was performed (**Scheme 4**). Their human monoamine oxidase A and B inhibitory potency was investigated. The IC₅₀ values of the most potent compounds were evaluated and *K_i* values were estimated using the Cheng–Prusoff equation [13]. A competitive-type inhibition for the most potent inhibitor was confirmed from the Lineweaver–Burk plots. The *K_i* value was in good agreement with the value deduced from the IC₅₀.

In this study, we also appraised the selectivity of the 5*H*-indeno[1,2-*c*]pyridazin-5-ones against human indoleamine 2,3-dioxygenase (hIDO) and *ralstonia metallidurans* tryptophan 2,3-dioxygenase (rmTDO), two enzymes involved, like MAO, in the metabolism of L-tryptophan (**Scheme 2**) [14]. It is known that IDO is overexpressed in a variety of diseases, including cancer and neurodegenerative disorders (e.g., Alzheimer's disease) [15–17]. Recently, it was shown that TDO is overexpressed in cancer [18]. IDO degrades indoleamines such as L-tryptophan, D-tryptophan,

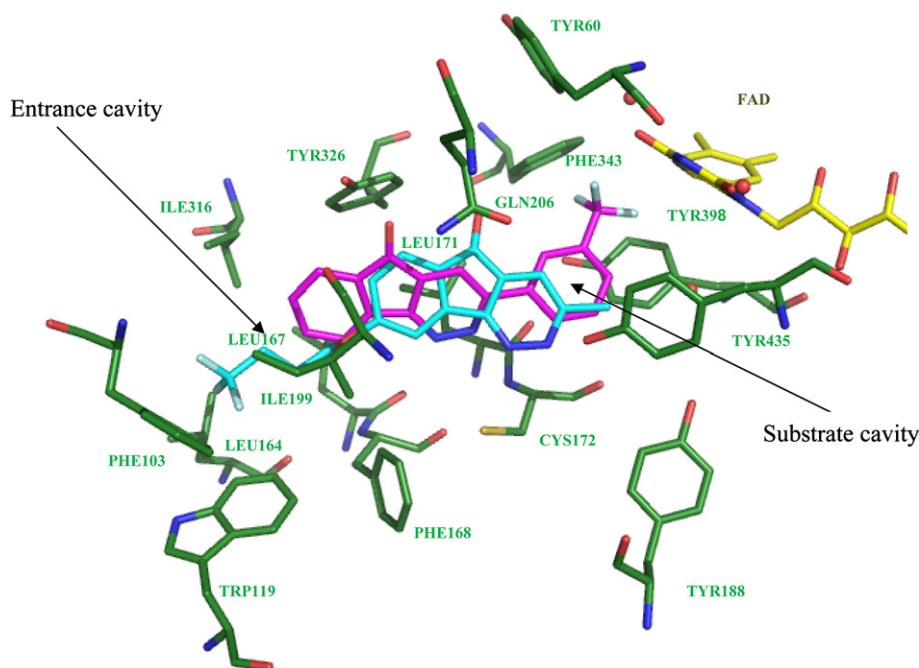
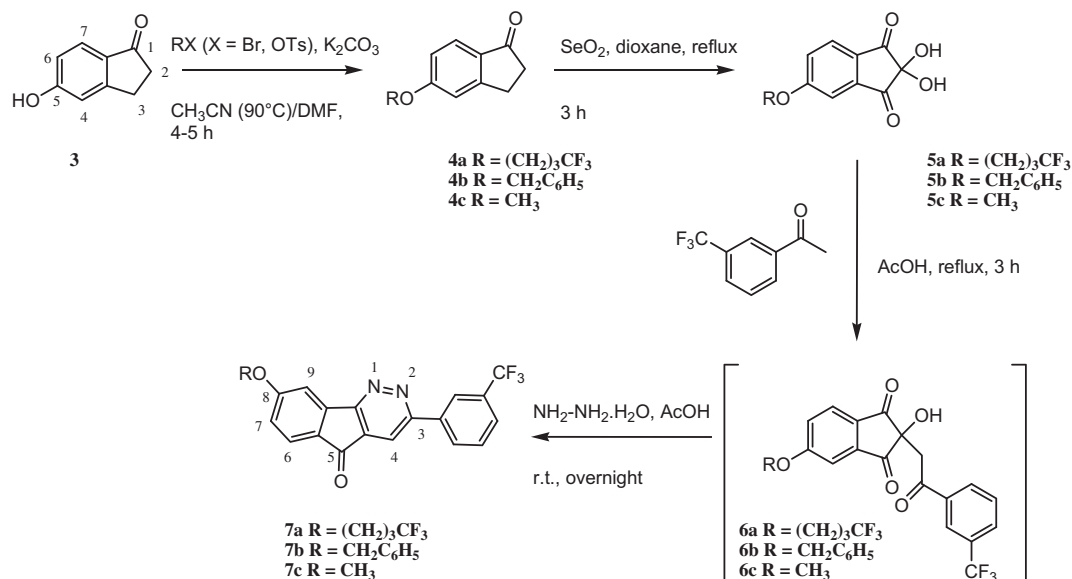


Fig. 1. Docking solutions of compounds **1** (magenta [9]) and **2** (cyan [12]) in the active site of hMAO-B (2V5Z.pdb). Only amino acids directly implicated in the active site are displayed and labelled in green. FAD is in yellow and the water molecules are displayed as red spheres.



Scheme 3. Synthetic pathway to 5H-indeno[1,2-c]pyridazin-5-one analogues **7a–c**.

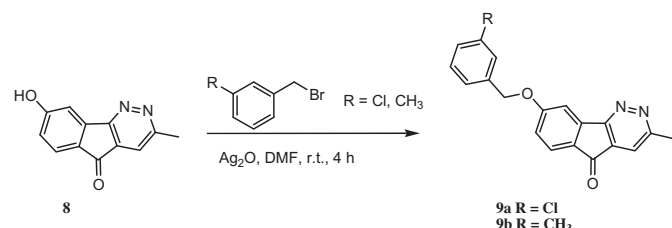
serotonin (MAO-A substrate) and tryptamine [19,20]. Of the dietary tryptophan that is not used in protein synthesis, most is metabolized by IDO/TDO through the kynurenine pathway, and a small amount of it is used to synthesize the neurotransmitter serotonin [14] (Scheme 2). Consequently, IDO and TDO play a critical role in determining the relative tryptophan flux in the serotonergic and kynurenine pathways [21]. Previous studies have shown the interest to use TDO inhibitors as serotonergic antidepressants [22]. So, this similarity in substrate between IDO and MAO, and the implication of IDO/TDO and MAO in the serotonergic and kynurenine pathways lead us to study the selectivity of our compounds against the three enzymes.

2. Results and discussion

2.1. Synthesis of 5H-indeno[1,2-c]pyridazin-5-one analogues

The strategy used to synthesize 8-(alkoxy)-3-(3'-(trifluoromethyl)phenyl)-5H-indeno[1,2-c]pyridazin-5-one derivatives (**7a–c**) is depicted in Scheme 3. This synthetic pathway follows a four steps procedure reported by our group from the common 5-hydroxy-1-indanone (**3**) intermediate [11,12].

5-Hydroxy-1-indanone (**3**) reacted with 1-tosyl-4,4,4-trifluorobutane in the presence of K₂CO₃ in acetonitrile for 4 h at 90 °C to give the 5-(4,4,4-trifluoromethylbutyloxy)-1-indanone (**4a**) in almost quantitative (96%) yield [11,12]. 5-Benzyloxy-1-indanone (**4b**) was obtained by reaction between the indanone (**3**), K₂CO₃, benzyl bromide in DMF for 5 h at room temperature in almost quantitative (90%) yield. 5-(Methoxy)-1-indanone (**4c**) is



Scheme 4. Synthetic pathway to 5H-indeno[1,2-c]pyridazin-5-one analogues **9a–b**.

commercially available. The alkoxyindanolins (**5a–c**) were synthesized by selenium dioxide oxidation of 5-alkoxy-1-indanones (**4a–c**) [11,12]. A dioxane solution of 5-alkoxy-1-indanone was mixed with selenium dioxide and refluxed for 3 h. This gave the 5-alkoxyindanolins **5a–c** in 73–81% yield. A solution of 5-alkoxyindanolin (**5a–c**) and 3'-(trifluoromethyl)acetophenone in acetic acid was refluxed for 3 h to give the intermediate aldol adduct (**6a–c**) [11,12,23]. After cooling to room temperature, the mixture reacted with hydrazine overnight. After purification on a silica gel column (dichloromethane 100% v), the 8-(alkoxy)-3-(3'-(trifluoromethyl)phenyl)-5H-indeno[1,2-c]pyridazin-5-one (**7a–c**) isomer was obtained in 39–46% yield. X-ray diffraction was used to unambiguously establish the position of the alkoxy group in the 8-position of the 5H-indeno[1,2-c]pyridazin-5-one moiety. ORTEP views of the conformations of **7a** and **7b**, with their atomic numbering scheme are depicted in Fig. 2. The synthesis of **9a–b** started from the phenol **8** (Scheme 4). Benzylation of **8** was achieved upon reaction with 1-(bromomethyl)-3-chlorobenzene or 1-(bromomethyl)-3-methylbenzene in the presence of silver oxide in DMF at room temperature for 4 h [11]. This provided **9a–b** in modest yields (6–15% yield). Again, X-ray diffraction was used to confirm the structure of **9a** (Fig. 2).

The structures of the synthesized compounds were determined by ¹H NMR, ¹³C NMR, mass spectrometry (MS) and their purity was assessed by elemental analyses.

2.2. Inhibitory potency of 5H-indeno[1,2-c]pyridazin-5-one analogues against MAO-A, MAO-B, IDO and TDO

First, the hMAO-A and hMAO-B inhibitory potency of the synthesized 5H-indeno[1,2-c]pyridazin-5-ones were assayed *in vitro* in triplicate at 10 μM using recombinant hMAO isoforms expressed in BTI (*Bacillus thuringiensis israelensis*) insect cells infected with baculovirus. The activity of MAO-A and MAO-B was determined by a luminescent method, according to a procedure developed by Valley et al. [24]. The K_i values of the most potent compounds were then estimated from the IC₅₀ values using the Cheng–Prusoff equation [13]. The results of MAO inhibition studies are reported in Tables 1 and 2. Compounds **7c** and **2** are known inhibitors of MAO-B [11,23] and were used as references. All the 5H-

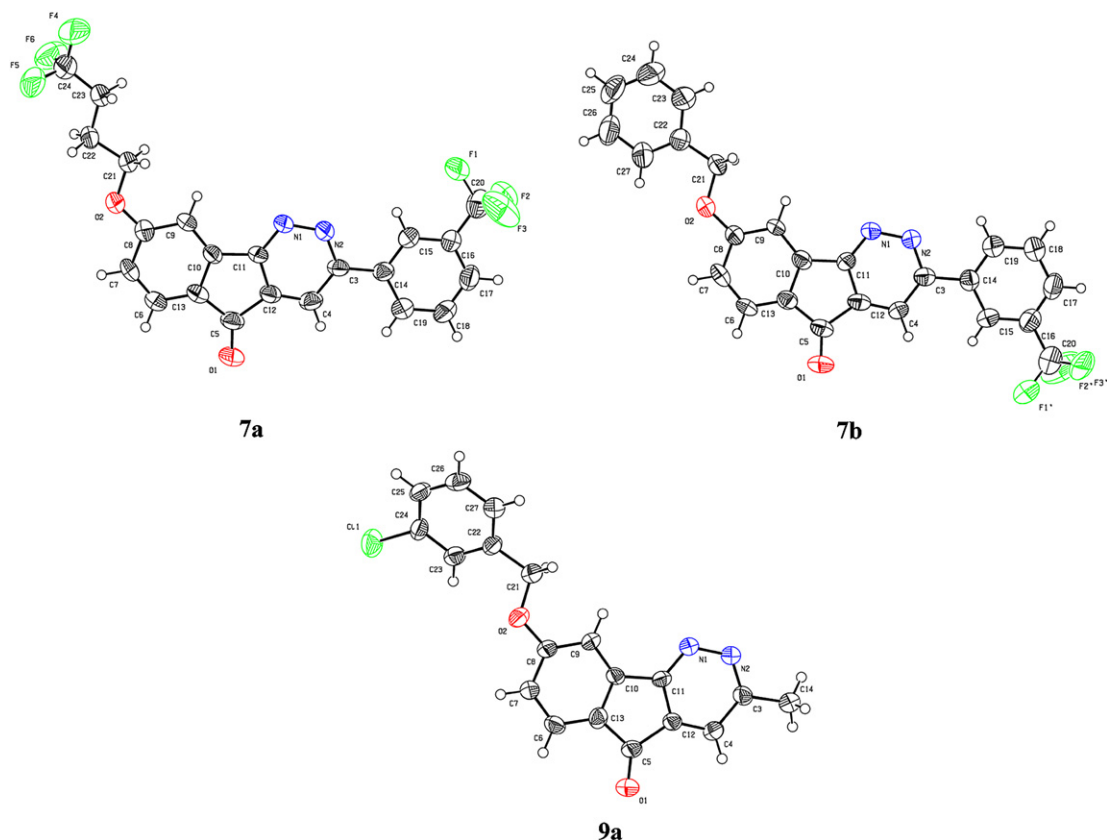


Fig. 2. The molecular structure of compounds **7a**, **7b** and **9a** showing the atom-numbering scheme. Displacement ellipsoids are drawn at the 50% probability level.

indeno[1,2-*c*]pyridazin-5-one analogues except **7b** present a higher inhibitory potency against MAO-B than MAO-A. The MAO inhibitory potency of these compounds proved to be highly dependent on the alkyl/aryl-substituent in the 3-position. Analogues with a *meta*-CF₃-phenyl group and a lipophilic group (methoxy, benzyloxy or trifluorobutyl) in the 3 and 8-positions respectively (**7a–c**) show moderate or no inhibition of MAO-B at 10 μM. Thus, the inhibitory activity of **7c** is not in agreement with the data reported by Frederick et al. [11]. However, it was evidenced in the literature that MAO affinity depends on species studied. In particular, Novaroli et al. have evidenced important species-dependent differences in MAO-B inhibitor specificity between human and rat for 5*H*-indeno[1,2-*c*]pyridazin-5-one derivatives [9]. Indeed, these derivatives show a greater inhibitory potency toward hMAO-B than toward rMAO-B (e.g., **1**, IC₅₀ rMAO-B = 280 nM and IC₅₀ hMAO-B = 8.5 nM) [9]. So, a difference of affinity between baboon and human enzymes can be conceived. In contrast, the substitution of *meta*-CF₃-phenyl group in the 3-position with a methyl group (**9a**, **9b** and **2**) leads to better inhibition (in the submicromolar range) of hMAO-B (Tables 1 and 2, Fig. 3). Compound **9a**, with a chlorine *meta*-substituted benzyloxy group, is the most active and selective within this series, with a *K_i* against MAO-B of 0.16 μM (Fig. 3).

To confirm the inhibition mode of MAO-B by **9a**, the Lineweaver–Burk plots were obtained from incubations at four different substrate concentrations with and without three different inhibitor concentrations. Lineweaver–Burk representation for **9a** on MAO-B demonstrates that its mechanism of inhibition is competitive (Fig. 4). The *K_i* value for the inhibition of MAO-B by **9a** was determined to be 0.11 μM what is in agreement with the *K_i* value estimated from the IC₅₀ value using the Cheng–Prusoff equation (Table 2) [13].

These results show that the substitution at both positions by lipophilic and bulky groups (**7a–c**) is not tolerated compared to analogues **9a**, **9b** and **2**. With the aim of understanding the role of an aryl group in the 3-position, molecular docking studies of compounds **9a** were performed and discussed in the next section.

The IDO and TDO inhibitory potencies of 5*H*-indeno[1,2-*c*]pyridazin-5-one analogues were assayed *in vitro* at 25 μM. The activity of IDO and TDO was determined by a colourimetric and fluorometric method respectively [25,26]. The results reveal that the synthesized 5*H*-indeno[1,2-*c*]pyridazin-5-one analogues display no inhibition or a moderate inhibition against IDO and TDO. The most effective one is 3-methyl-8-*meta*-methylbenzyloxy-5*H*-indeno[1,2-*c*]pyridazin-5-one (**9b**) which displays a 66% inhibition of TDO. So, 5*H*-indeno[1,2-*c*]pyridazin-5-one derivatives display a higher activity and selectivity against hMAO-B.

2.3. Molecular docking studies of compound **9a** against MAO-B

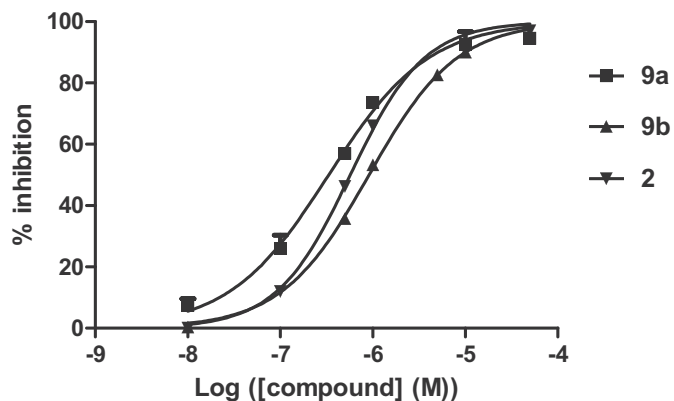
While the 5*H*-indeno[1,2-*c*]pyridazin-5-one derivatives differently substituted in the 3- and 8-positions investigated here were weak MAO-A, IDO and TDO inhibitors, some were found to be potent inhibitors of MAO-B. Among these, compound **9a**, was the most potent and selective MAO-B inhibitor. To gain insight into the potential binding mode of **9a** in the active site of MAO-B, molecular docking studies were performed with the crystallographic structure of hMAO-B in complex with safinamide (2V5Z.pdb) as receptor model [27]. With the exception of three highly conserved water molecules all buried near the flavin adenine dinucleotide cofactor (FAD) in the active site, the other crystallized water molecules were deleted from the protein model [9]. In MAO-B, two distinct cavities

Table 1Structure and inhibitory potency of synthesized 5*H*-indeno[1,2-*c*]pyridazin-5-one derivatives against hMAO-A, hMAO-B, hIDO and rmTDO.

Compound	Structure	Inhibition percentage ^a			
		hMAO-A at 10 μ M	hMAO-B at 10 μ M	hIDO at 25 μ M	rmTDO at 25 μ M
7a		NI ^b	57% \pm 10	NI	20% \pm 3
7b		10% \pm 10	7% \pm 3	17% \pm 1	NI
7c		NI	36% \pm 2	NI	18% \pm 3
9a		15% \pm 5	93% \pm 4	25% \pm 3	19% \pm 6
9b		17% \pm 1	90% \pm 0	14% \pm 2	66% \pm 4
2		NI	92% \pm 0	19% \pm 2	31% \pm 4

^a Inhibition percentages are expressed as mean with \pm SD in brackets ($n = 3$).^b NI: no inhibition at 10 μ M and 25 μ M on MAO-A/MAO-B and IDO/TDO respectively.**Table 2** K_i values deduced from IC_{50} /measured for hMAO-B for compounds 9a, 9b and 2.

Compound	K_i (μ M)	
	Deduced from IC_{50} ^a	Measured ^b
9a	0.16 (0.14–0.19)	0.11 \pm 0.01
9b	0.48 (0.42–0.55)	
2	0.28 (0.26–0.30)	

^a K_i values are estimated from the experimentally measured IC_{50} values using the Cheng–Prusoff equation and are expressed as mean within brackets 95% confidence intervals ($n = 3$).^b K_i value is measured from the Lineweaver–Burk representation and is expressed as the mean \pm SD ($n = 3$).**Fig. 3.** Dose–response curve of compounds 9a (■), 9b (▲) and 2 (▼) on hMAO-B. Inhibition percentages are shown as mean \pm SD with $n = 3$.

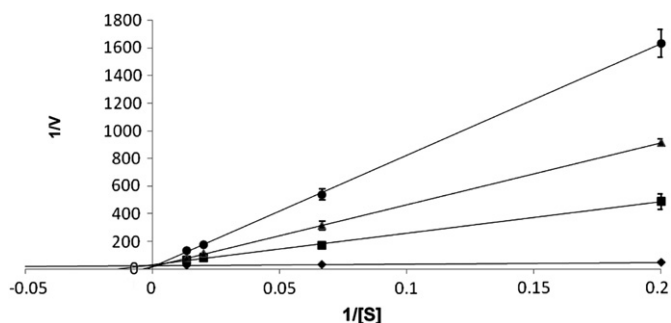


Fig. 4. Lineweaver–Burk plots of the inhibition of recombinant human MAO-B by **9a**. The lines were constructed in the absence (◆) and presence of 2 μM (■), 5 μM (▲) and 15 μM (●) of **9a** with $n = 3$.

can be found within the binding site; an “entrance cavity” and a “substrate cavity” (Fig. 5a). The entrance cavity is connected to the outside of the protein whereas the substrate cavity is located in the vicinity of FAD. Both cavities are separated by ILE199 and TYR326 acting as a gate, protecting the catalytic region from the outside. The ILE199 side chain is the latch separating both cavities and displayed in Fig. 5a in the “open” position, allowing the 5*H*-indeno [1,2-*c*]pyridazin-5-one derivatives to reach both cavities.

The docking solutions were ranked according to their respective Goldscore values. Analysis of the binding mode for compound **9a** (Fig. 5a) revealed that 5*H*-indeno[1,2-*c*]pyridazin-5-one core is located in the vicinity of the FAD cofactor with the C-8 side chain projecting towards the entrance cavity of MAO-B. The substrate cavity is mainly hydrophobic, the only hydrophilic region being located between TYR398, TYR435 and flavin which form an aromatic cage. The examination of the molecular electrostatic potential (MEP)

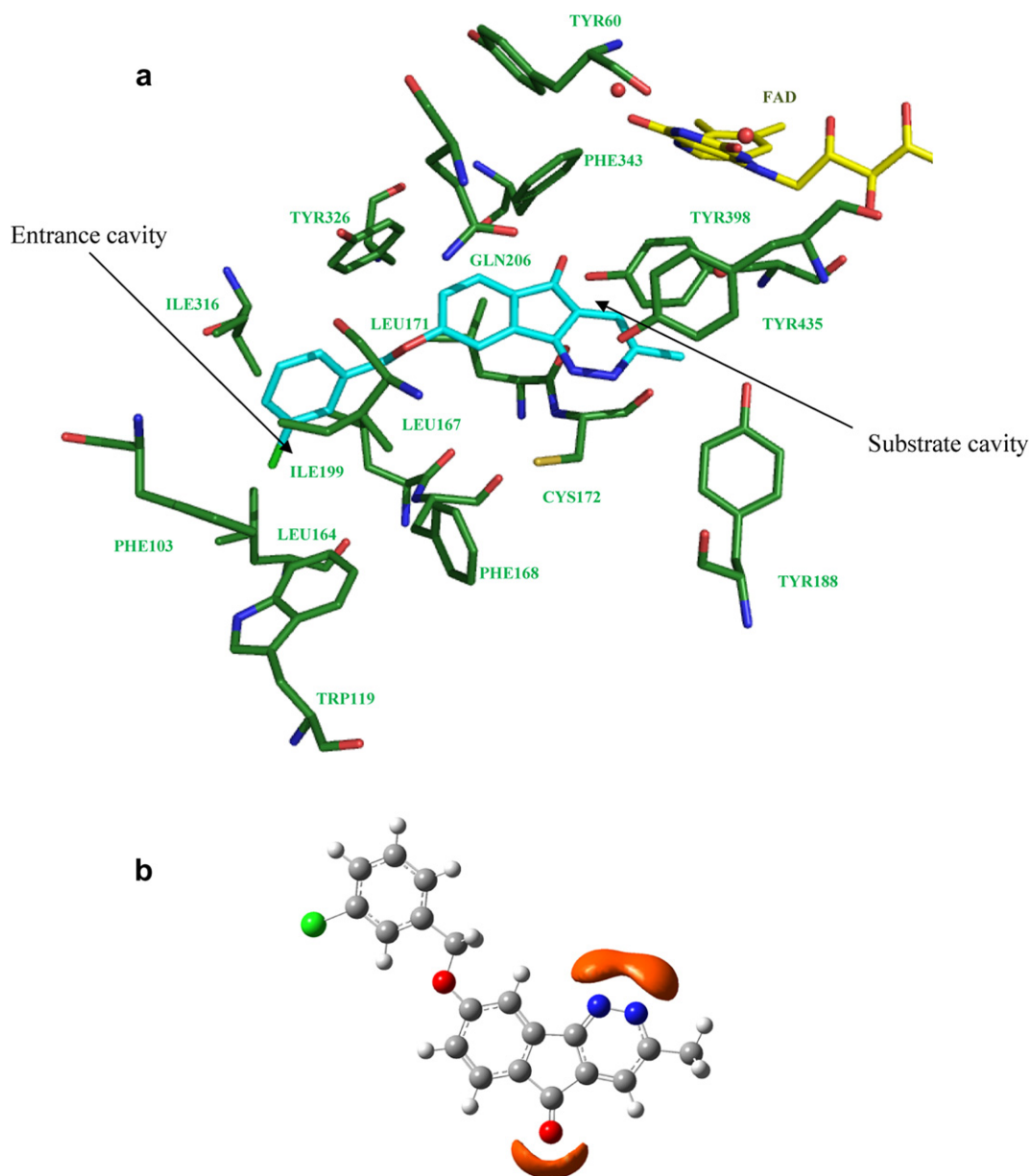


Fig. 5. a) Simulated binding mode of **9a** in the active site of hMAO-B (2V5Z.pdb). Only amino acids directly implicated in the active site are displayed and labelled (in green). Compound **9a** is in cyan. FAD is in yellow. The water molecules in the active site are displayed as red spheres. (b) Attractive molecular electrostatic potential (isovalue for surfaces = 10 kcal/mol) calculated around compound **9a**. (PBE1PBE, 6-311G**).(For interpretation of the references to colour in this figure legend, the reader is referred to the web version of this article.)

distribution for compound **9a** shows the presence of two large attractive zones around the 5*H*-indeno[1,2-*c*]pyridazin-5-one ring (Fig. 5b). The first one is centred on the carbonyl and the second one is centred on the endocyclic hydrazine. So, it is not surprising to observe that both regions are located within the hydrophilic region of the MAO-B substrate cavity. Furthermore, the 5*H*-indeno[1,2-*c*]pyridazin-5-one ring is stabilized by π - π interactions with TYR398 and TYR435. The binding mode adopted by compound **9a** allows the *meta*-chlorobenzoyloxy side chain to settle within the entrance cavity lined with hydrophobic amino acid residues. This hydrophobic pocket is coated by PHE103, TRP119, LEU164, LEU167, PHE168, and ILE316. Interestingly, the introduction of a chlorine atom on the benzyl ring (**9a**, $K_i = 0.16 \mu\text{M}$) increases the inhibitory potency against MAO-B compared to the derivative bearing a methyl group (**9b**, $K_i = 0.48 \mu\text{M}$). Previous studies have shown that addition of a chlorine substituent on the phenyl group side chain enhance the lipophilicity of the inhibitor, and therefore its affinity and its selectivity against MAO-B establishing Van der Waals interactions in the hydrophobic entrance cavity [28]. Compound **2** ($K_i = 0.28 \mu\text{M}$) with the trifluorobutyloxy group displays a similar inhibition compared to **9a**. The methyl group in the 3-position is stabilized within the hydrophobic cage formed by TYR398, TYR435 and FAD. The substrate cavity being more sterically constrained than the entrance cavity, the *meta*-CF₃-phenyl group of compounds **7a–c** cannot accommodate into the substrate cavity without modifying the binding mode of 5*H*-indeno[1,2-*c*]pyridazin-5-one ring. So, these observations may explain the reduced inhibition of compounds **7a–c** compared to **9a–b** and **2**.

3. Conclusion

In order to design new, selective, and more potent MAO-B inhibitors, a series of 5*H*-indeno[1,2-*c*]pyridazin-5-one derivatives substituted both in the 3- and 8-positions by lipophilic groups has been synthesized. X-ray diffraction technique was used to unambiguously establish the position of the alkoxy group on the phenyl ring of the 5*H*-indeno[1,2-*c*]pyridazin-5-one moiety. Their inhibitory potency has been evaluated by a luminescent test on hMAO-A and -B. In this study, the selectivity of our series was also established against two enzymes (IDO and TDO) involved in the serotonergic and kynurenine pathways. IDO and TDO inhibitory potency of 5*H*-indeno[1,2-*c*]pyridazin-5-one analogues was determined by a colourimetric and fluorometric method, respectively. The results show that, at 25 μM , the synthesized 5*H*-indeno[1,2-*c*]pyridazin-5-ones display no inhibition or a moderate inhibition of IDO and/or TDO. The most effective compound is 3-methyl-8-*meta*-methylbenzoyloxy-5*H*-indeno[1,2-*c*]pyridazin-5-one (**9b**) with 66% inhibition of TDO. All compounds, except **7b**, displayed a higher activity and selectivity against MAO-B. 3-Methyl-8-*meta*-chlorobenzoyloxy-5*H*-indeno[1,2-*c*]pyridazin-5-one **9a**, is the most active and selective within this series, with a K_i against MAO-B of 0.11 μM . Replacement of the methyl moiety in the 3-position by a lipophilic group like a *meta*-CF₃-phenyl group (**7a–c**) abolishes the inhibitory potency against MAO-B. So, the substitution of the 5*H*-indeno[1,2-*c*]pyridazin-5-one core in the 3-position dramatically influences the MAO-inhibiting properties of these compounds. Docking simulations of compound **9a** in hMAO-B suggest that the 5*H*-indeno[1,2-*c*]pyridazin-5-one core incorporates into the substrate cavity with the *meta*-chlorobenzoyloxy side chain extending towards a hydrophobic pocket of the entrance cavity space.

Acknowledgements

J. Reniers and R. Frederick thank the Belgian National Fund for Scientific Research (F.N.R.S.) for financial support, Ms. Bernadette

Norberg for her assistance with the XRD analysis and Ms. Jenny Pouyez for her assistance with the IDO inhibition assay.

Appendix. Supplementary material available

Chemicals and instrumentation; Synthesis of 5*H*-indeno[1,2-*c*]pyridazin-5-ones; Single crystal X-ray crystallographic data of 5*H*-indeno[1,2-*c*]pyridazin-5-one derivatives (**7a**, **7b** and **9a**); Enzymatic assays (MAO-A and -B, IDO and TDO); Molecular docking; Molecular electrostatic potential (MEP) calculation.

CCDC-813566, CCDC-813564 and CCDC-813565 contain the supplementary crystallographic data for this paper. These data can be obtained free of charge from The Cambridge Crystallographic Data Centre via www.ccdc.cam.ac.uk/data_request/cif.

Appendix. Supplementary material

Supplementary data related to this article can be found online at doi:10.1016/j.ejmech.2011.09.042.

References

- [1] W. Weyler, Y.P. Hsu, X.O. Breakefield, Biochemistry and genetics of monoamine oxidase, *Pharmacol. Ther.* 47 (1990) 391–417.
- [2] D.E. Edmondson, A. Mattevi, C. Binda, M. Li, F. Hubalek, Structure and mechanism of monoamine oxidase, *Curr. Med. Chem.* 11 (2004) 1983–1993.
- [3] J. Grimmsby, N.C. Lan, R. Neve, K. Chen, J.C. Shih, Tissue distribution of human monoamine oxidase A and B mRNA, *J. Neurochem.* 55 (1990) 1166–1169.
- [4] C.W. Abell, S.W. Kwan, Molecular characterization of monoamine oxidases A and B, *Prog. Nucleic Acid Res. Mol. Biol.* 65 (2001) 129–156.
- [5] K.F. Tipton, S. Boyce, J. O'Sullivan, G.P. Davey, J. Healy, Monoamine oxidases: certainties and uncertainties, *Curr. Med. Chem.* 11 (2004) 1965–1982.
- [6] M. Yamada, H. Yasuhara, Clinical pharmacology of MAO inhibitors: safety and future, *Neurotoxicology* 25 (2004) 215–221.
- [7] B. Drukarch, F.L. van Muiswinkel, Drug treatment of Parkinson's disease. Time for phase II, *Biochem. Pharmacol.* 59 (2000) 1023–1031.
- [8] A.H. Schapira, Treatment options in the modern management of Parkinson disease, *Arch. Neurol.* 64 (2007) 1083–1088.
- [9] L. Novaroli, A. Daina, E. Favre, J. Bravo, A. Carotti, F. Leonetti, M. Catto, P.A. Carrupt, M. Reist, Impact of species-dependent differences on screening, design, and development of MAO B inhibitors, *J. Med. Chem.* 49 (2006) 6264–6272.
- [10] A. Carotti, M. Catto, F. Leonetti, F. Campagna, R. Soto-Otero, E. Mendez-Alvarez, U. Thull, B. Testa, C. Altomare, Synthesis and monoamine oxidase inhibitory activity of new pyridazine-, pyrimidine- and 1,2,4-triazine-containing tricyclic derivatives, *J. Med. Chem.* 50 (2007) 5364–5371.
- [11] R. Frederick, W. Dumont, F. Ooms, L. Aschenbach, C.J. Van der Schyf, N. Castagnoli, J. Wouters, A. Krief, Synthesis, structural reassignment, and biological activity of type B MAO inhibitors based on the 5*H*-indeno[1,2-*c*]pyridazin-5-one core, *J. Med. Chem.* 49 (2006) 3743–3747.
- [12] F. Ooms, R. Frederick, F. Durant, J.P. Petzer, N. Castagnoli, C.J. Van der Schyf, J. Wouters, Rational approaches towards reversible inhibition of type B monoamine oxidase. Design and evaluation of a novel 5*H*-Indeno[1,2-*c*]pyridazin-5-one derivative, *Bioorg. Med. Chem. Lett.* 13 (2003) 69–73.
- [13] Y. Cheng, W.H. Prusoff, Relationship between the inhibition constant (K_i) and the concentration of inhibitor which causes 50 per cent inhibition (I_{50}) of an enzymatic reaction, *Biochem. Pharmacol.* 22 (1973) 3099–3108.
- [14] T.W. Stone, L.G. Darlington, Endogenous kynurenes as targets for drug discovery and development, *Nat. Rev. Drug Discov.* 1 (2002) 609–620.
- [15] K. Matsuno, K. Takai, Y. Isaka, Y. Unno, M. Sato, O. Takikawa, A. Asai, S-benzylisothiourea derivatives as small-molecule inhibitors of indoleamine-2,3-dioxygenase, *Bioorg. Med. Chem. Lett.* 20 (2010) 5126–5129.
- [16] C. Uyttenhove, L. Pilotte, I. Theate, V. Stroobant, D. Colau, N. Parmentier, T. Boon, B.J. Van den Eynde, Evidence for a tumoral immune resistance mechanism based on tryptophan degradation by indoleamine 2,3-dioxygenase, *Nat. Med.* 9 (2003) 1269–1274.
- [17] G.J. Guillemain, B.J. Brew, C.E. Noonan, O. Takikawa, K.M. Cullen, Indoleamine 2,3-dioxygenase and quinolinic acid immunoreactivity in Alzheimer's disease hippocampus, *Neuropathol. Appl. Neurosci.* 31 (2005) 395–404.
- [18] B. Van Den Eynde, L. Pilotte, E. De Plaen, Tryptophan catabolism in cancer treatment and diagnosis, *PCT Int. Appl.* (2010).
- [19] T. Shimizu, S. Nomiyama, F. Hirata, O. Hayaishi, Indoleamine 2,3-dioxygenase. Purification and some properties, *J. Biol. Chem.* 253 (1978) 4700–4706.
- [20] U.F. Rohrig, L. Awad, A. Grosdidier, P. Larrieu, V. Stroobant, D. Colau, V. Cerundolo, A.J. Simpson, P. Vogel, B.J. Van den Eynde, V. Zoete, O. Michielin, Rational design of indoleamine 2,3-dioxygenase inhibitors, *J. Med. Chem.* 53 (2010) 1172–1189.

- [21] D. Batabyal, S.R. Yeh, Human tryptophan dioxygenase: a comparison to indoleamine 2,3-dioxygenase, *J. Am. Chem. Soc.* 129 (2007) 15690–15701.
- [22] M. Salter, Selective inhibitors of tryptophan 2,3-dioxygenase and combined inhibitors of tryptophan 2,3-dioxygenase and 5-HT reuptake as novel serotonergic antidepressants, *CNS Drug Rev.* 2 (1996) 127–143.
- [23] S. Kneubuhler, U. Thull, C. Altomare, V. Carta, P. Gaillard, P.A. Carrupt, A. Carotti, B. Testa, Inhibition of monoamine oxidase-B by 5*H*-indeno [1,2-*c*]pyridazines: biological activities, quantitative structure-activity relationships (QSARs) and 3D-QSARs, *J. Med. Chem.* 38 (1995) 3874–3883.
- [24] M.P. Valley, W. Zhou, E.M. Hawkins, J. Shultz, J.J. Cali, T. Worzella, L. Bernad, T. Good, D. Good, T.L. Riss, D.H. Klaubert, K.V. Wood, A bioluminescent assay for monoamine oxidase activity, *Anal. Biochem.* 359 (2006) 238–246.
- [25] A. Matin, I.M. Streete, I.M. Jamie, R.J. Truscott, J.F. Jamie, A fluorescence-based assay for indoleamine 2,3-dioxygenase, *Anal. Biochem.* 349 (2006) 96–102.
- [26] O. Takikawa, T. Kuroiwa, F. Yamazaki, R. Kido, Mechanism of interferon-gamma action. Characterization of indoleamine 2,3-dioxygenase in cultured human cells induced by interferon-gamma and evaluation of the enzyme-mediated tryptophan degradation in its anticellular activity, *J. Biol. Chem.* 263 (1988) 2041–2048.
- [27] C. Binda, J. Wang, L. Pisani, C. Caccia, A. Carotti, P. Salvati, D.E. Edmondson, A. Mattevi, Structures of human monoamine oxidase B complexes with selective noncovalent inhibitors: safinamide and coumarin analogs, *J. Med. Chem.* 50 (2007) 5848–5852.
- [28] L.H. Prins, J.P. Petzer, S.F. Malan, Inhibition of monoamine oxidase by indole and benzofuran derivatives, *Eur. J. Med. Chem.* 45 (2010) 4458–4466.